Diffusion tensor imaging reveals changes in the adult rat brain following long-term and passive moderate acoustic exposure

Sherwin Abdoli,[1] Leon C. Ho,[2,a)] Jevin W. Zhang,[2,a)] Celia M. Dong,[2,a)] Condon Lau,[3,b)] and Ed X. Wu[2,a)]

[1]*Keck School of Medicine, University of Southern California, 1975 Zonal Avenue, Los Angeles, California 90033, USA*

[2]*Laboratory of Biomedical Imaging and Signal Processing, LB1037, 10/F, Laboratory Block, The University of Hong Kong, 21 Sassoon Road, Pokfulam, Hong Kong, China*

[3]*Department of Physics and Materials Science, G6702, 6/F, Academic Building 1, City University of Hong Kong, Tat Chee Avenue, Kowloon, Hong Kong, China*

(Received 16 May 2016; revised 1 December 2016; accepted 2 December 2016; published online 30 December 2016)

This study investigated neuroanatomical changes following long-term acoustic exposure at moderate sound pressure level (SPL) under passive conditions, without coupled behavioral training. The authors utilized diffusion tensor imaging (DTI) to detect morphological changes in white matter. DTIs from adult rats ($n = 8$) exposed to continuous acoustic exposure at moderate SPL for 2 months were compared with DTIs from rats ($n = 8$) reared under standard acoustic conditions. Two distinct forms of DTI analysis were applied in a sequential manner. First, DTI images were analyzed using voxel-based statistics which revealed greater fractional anisotropy (FA) of the pyramidal tract and decreased FA of the tectospinal tract and trigeminothalamic tract of the exposed rats. Region of interest analysis confirmed ($p < 0.05$) that FA had increased in the pyramidal tract but did not show a statistically significant difference in the FA of the tectospinal or trigeminothalamic tract. The results of the authors show that long-term and passive acoustic exposure at moderate SPL increases the organization of white matter in the pyramidal tract. © *2016 Acoustical Society of America*.
[http://dx.doi.org/10.1121/1.4972300]

[AKCL] Pages: 4540–4547

I. INTRODUCTION

The deleterious effects of acoustic exposure at high sound pressure levels (SPLs) have been well-studied. Acoustic exposure at high SPL has been shown to permanently damage the auditory system and even cause psychological disturbances through the resulting tinnitus.[1–4] Likewise, auditory deprivation has been shown to cause atrophy of the auditory system and prevent the development of higher-order thinking.[5–7] In contrast to the extensive research investigating the effects of acoustic exposure at high SPL and auditory deprivation, relatively little research has been done investigating the effects of long-term acoustic exposure at moderate SPL (below levels required to elevate the hearing threshold) to which many individuals are exposed.[8,9] Long-term acoustic exposure at moderate SPL coupled with behavioral training has been shown to increase auditory discrimination. Rats conditioned to respond to acoustic stimulus based on its frequency demonstrated an extended representation of frequency tonotopic maps while rats conditioned to respond based on acoustic intensity demonstrated an increased proportion of nonmonotonic intensity response profiles.[10]

Considering how readily sensory systems adapt to environmental conditions, it is likely that the auditory system also adapts to long-term and passive (no behavioral training) acoustic exposure at moderate SPL.[11] At the cellular level, the adaptive ability of the auditory system can be demonstrated through the gradual atrophy of spiral ganglion following ototoxicity and their continued survival if electrically stimulated.[12] These simple cellular adaptations have complex manifestations in the central nervous system. In a study with exposure variables similar to ours, adult cats passively exposed to a continuous 65 dB pulse train demonstrated a decreased ability to discriminate between auditory stimuli and degradation in cortical temporal processing.[13] Prior functional magnetic resonance imaging studies demonstrated that prolonged exposure to a similar 65 dB pulse train leads to subcortical functional changes in adult rats.[14,15]

Juvenile rats, whose developing brains are more plastic than those of adult rats, demonstrate impaired hearing function as adults if they are reared in environments with long-term and passive acoustic exposure. Rats which were postnatally exposed to 80 dB SPL interrupted white noise for 8 h a day for 2 weeks demonstrated a significantly decreased minimum threshold, first spike latency, dynamic range, and slope of the rate-level functions of cortical neurons 7 weeks later in comparison to adult rats reared in standard housing. In comparison, adult rats exposed to the same long-term and passive acoustic exposure did not have a significant change of sound level processing by the auditory cortical neurons.[16] Another study found that long-term and passive acoustic exposure caused attenuated spatial sensitivity of *A*1 neurons

[a)]Also at Department of Electrical and Electronic Engineering, The University of Hong Kong, Hong Kong, China.
[b)]Electronic mail: condon.lau@cityu.edu.hk

in postnatal rats linked with a corresponding expression of GAD65 and GABAA receptor subunits in the auditory cortex indicating adverse effects on the maturation of cortical GABAergic inhibition.[17] The NMDA-2A and 2B receptors, receptors which have an inhibitory effect on sensory stimuli, have been shown to be expressed at increased levels in rats which, during development, received long-term and passive acoustic exposure and subsequently demonstrated poor temporal processing acuity as adults.[18]

There have been behavioral, pathophysiological, and electrophysiological studies on the effect of long-term and passive acoustic exposure at moderate SPL on the developed brain. Investigating the morphological changes associated with these behavioral and electrophysiological changes is essential to understanding the mechanisms through which the auditory system adapts and gauging the extent of the adaptations.[19,20] Diffusion tensor imaging (DTI) is ideal for studying subtle changes in brain morphology as it can reveal changes in the organization of white matter tracts in a manner not readily observable by regular magnetic resonance imaging (MRI), which can only reveal extensive atrophy or hypertrophy, such as those seen in extreme cases of acoustic exposure at high SPL or auditory deprivation.[21,22]

Prior studies have successfully utilized DTI to observe white matter degradation following sensorineural hearing loss and tinnitus.[23–25] Hearing loss and blast-induced tinnitus in rats have been associated with decreases in fractional anisotropy (FA) and increases in mean diffusivity (MD), which are indications of decreased axonal integrity, in the inferior colliculus and medial geniculate body.[26–29] Patients with sensorineural hearing loss were found to have decreased FA and increased radial diffusivity (RD) in the lateral lemniscus and inferior colliculus.[30] Likewise, patients with congenital cochlear nerve deficiency were found to have decreased FA and increased MD on both the ipsilateral and contralateral sides of the nerve.[31]

In this study, we identify changes in the white matter tracts of adult rats caused by long-term and passive acoustic exposure at moderate SPL. While the DTI-based auditory system studies we discussed earlier preselected a few structures for subsequent region of interest (ROI) analysis, we perform voxel-based statistics (VBS) analysis of the entire brain first ensuring that no structures are overlooked and to increase specificity. VBS is used to compare DTI images from rats exposed to long-term and passive acoustic exposure at moderate SPL with DTI images from rats reared in a standard environment. We perform ROI analysis on structures indicated by VBS to increase the specificity of our test.

II. METHODS

A. Animal preparation

All aspects of this study were approved by the Animal Ethics Committee of the City University of Hong Kong and the Committee on the Use of Live Animals in Teaching and Research of the University of Hong Kong. Normal female Sprague–Dawley rats (3 months of age, $n = 16$) were used in this study. The subjects were reared in two chronologically consecutive sets. Each set had four noise-exposed subjects and four control subjects. Noise exposed subjects were housed together in a cage with a MF1 speaker (Tucker-Davis Technologies, Alachua, FL) placed on top. The speaker's output was calibrated and checked regularly using the microphone. Control subjects were housed in a separate room with similar layout. Background noise in the rooms was less than 40 dB total SPL. All rats were housed in pairs, exposed to 12-h light/dark cycles, and received standard food and water *ad libitum*. Acoustic exposure began when the exposure rats were 3 months old. At the same time, the control rats continued to be housed in standard acoustic conditions. The exposure was a 5 Hz pulse train repeated 24 h/day for 2 months. Each pulse had duration of 50 ms, was 65 dB total SPL, and was low-pass filtered at 30 kHz (Fig. 1). This rat acoustic exposure model was chosen because it had been used in comparable behavioral and electrophysiological studies and demonstrated that it does not shift auditory brainstem response (ABR) thresholds. ABR testing did not observe any clinically significant hearing threshold shift following exposure, as shown in the supplementary material,[32] consistent with ABR testing performed by Zhou *et al.*[13]

Imaging was performed at 5 months of age. Each rat was anesthetized with 3% isoflurane (mixed with room air) then anesthesia was maintained with 1.5%–2% isoflurane throughout the course of setup and scanning. The rat was placed in the prone position on a body holder with a head motion restricting nose cone and tooth bar. Respiration rate, heart rate, saturation of peripheral oxygen, and rectal temperature were continuously monitored (SA-Instruments, Stony Brook, NY).

B. MRI protocol

The rats were scanned using a 7 T MRI scanner with a maximum gradient of 360 mT/m (PharmaScan, Bruker BioSpin, Germany). A birdcage transmit-only coil with 72 mm inner diameter was used in combination with an actively decoupled receive-only quadrature surface coil. Once the animal was properly anesthetized and positioned in the scanner, scout images were acquired to determine the coronal and sagittal planes of the brain. Twelve 1.0 mm thick slices, spaced 0.18 mm apart, were positioned by referencing the rat brain atlas such that the fourth slice was centered on the inferior colliculus (Fig. 2).[33] Multiple redundant diffusion-weighted images were acquired using a spin-echo 4-shot echo planar imaging sequence with 30 diffusion gradient directions and b-value $= 1000\ \mathrm{s/mm^2}$. Five images without diffusion sensitization ($b = 0.0\ \mathrm{ms/\mu m^2}$, $b0$ images) were also acquired. Images with motion artifacts were discarded. The imaging parameters were: repetition time/echo time $= 3000/31.6$ ms, $\delta/\Delta = 5/17$ ms, field of view $= 3.2 \times 3.2\ \mathrm{cm^2}$, data matrix $= 128 \times 128$, up-sampled data matrix $= 256 \times 256$, cropped data matrix $= 128 \times 128$, and number of excitements $= 4$. Anatomical images were acquired with rapid acquisition with refocusing echoes (RARE). The imaging parameters were RARE factor $= 8$, repetition time/echo time $= 4200/32$, field of view $= 3.2 \times 3.2\ \mathrm{cm^2}$, data matrix $= 256 \times 256$.

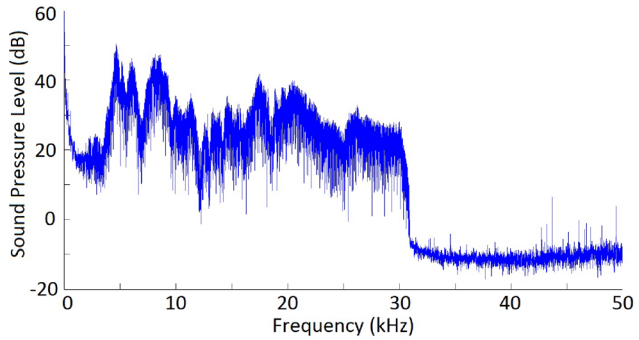

FIG. 1. (Color online) Acoustic power spectrum of a pulse of the exposure. The exposure was a 5 Hz pulse train repeated 24 h/day for 2 months. Each pulse had duration of 50 ms, was 65 dB total SPL, and was low-pass filtered at 30 kHz. Background noise was less than 40 dB total SPL. The spectrum was recorded with a high frequency microphone (M50, Earthworks, Chesterfield, MO).

C. Data analysis

The diffusion-weighted images and *b*0 images of the 16 rats were realigned and normalized to the *b*0 image of a template rat (SPM8, Wellcome Trust Centre, Oxford, United Kingdom). DTI index maps from each trial were generated by a custom MATLAB program. MD, FA, axial diffusivity (AD), and RD maps were calculated with *b*-values 0 versus 1.0 ms/μm^2 and 0 versus 0.3 ms/μm^2, respectively, as previously described.[34] A map of color-coded directionality was generated, in which the color codes for the principal eigenvector orientation while the contrast is weighted with FA.

A voxel-wise *t*-test was performed between the FA maps of the control and exposure rats to generate VBS. The first and last slices were excluded in order to avoid truncation artifacts. VBS clusters were considered significant if there were at least 50 contiguous, as defined by a common surface across the same or adjacent slices, significant voxels with $p < 0.0005$. The structures indicated by clusters were identified using the rat neuroanatomy atlas.

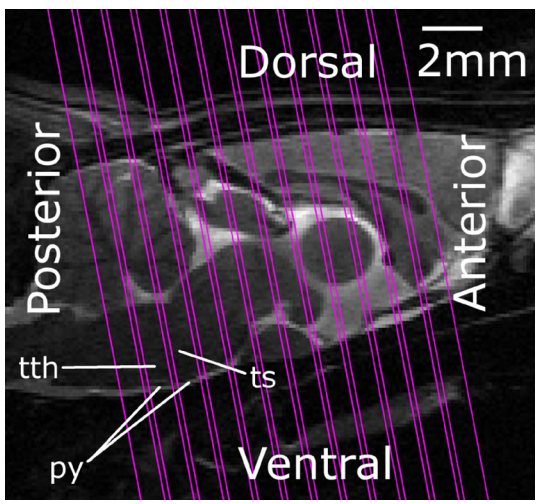

FIG. 2. (Color online) Twelve 1.0 mm thick slices, spaced 0.18 mm apart, were positioned by referencing the rat brain atlas (Ref. 33) such that the fourth slice was centered on the inferior colliculus (IC). The pyramidal tract (py), tectospinal tract (ts), and the trigeminothalamic tract (tth) are labelled. The positions of the slices, from caudal to rostral, are represented by pink boxes.

ROI analysis was used to confirm that the structures identified by VBS were not significantly affected by normalization, registration, or other processing errors. Due to its confirmatory purpose, the ROI analysis was done in a conservative manner on unnormalized images. For each VBS identified structure, left and right hemisphere ROIs were drawn (Fig. 3). The ROIs were drawn such that they would be exclusive to the identified structure regardless of which rat they were applied to resulting in ROIs that were slightly smaller than the actual structure but still representative of the structure's general shape and size. All ROIs were of identical shape, size, and the left and right ROIs were always placed along the same horizontal axis. The only variation between the subjects was the distance between the right and left ROI. The atlas was used to determine anatomical landmarks, such as the edge of the brain as the starting point of the pyramidal tract, to serve as guidelines for placement of the ROIs. Once the ROIs were placed, FA, MD, RD, and AD values were recorded for the left and right structures. Values were recorded from the left and right sides to ensure that changes were occurring bilaterally.

Following ROI analysis, tractography was performed to ensure that ROIs drawn corresponded to the intended white matter structures. The ROI for the pyramidal tract was placed on the second coronal slice of the template and then used to generate tracks. Tracking was performed on a voxel-by-voxel basis by continuously following the orientation of the tensor first eigenvector. All fiber bundles passing through the ROI on the second coronal slice which had a minimum FA threshold of 0.4 were followed until their FA was under 0.2 or the turning angle was greater than 60° (Fig. 4).

III. RESULTS

The rats in the exposure group received long-term acoustic exposure at moderate SPL for 2 months (Fig. 1). The rats were scanned with a 7 T MRI scanner and twelve 1.0 mm thick slices, spaced 0.18 mm apart, were positioned with the fourth slice centered on the inferior colliculus (Fig. 2). VBS were used to identify structures that had undergone significant changes and for each identified structure, a ROI analysis was performed (Fig. 3). Figure 5 shows the results

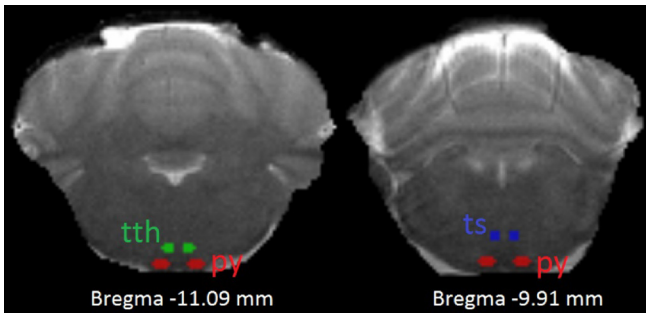

FIG. 3. (Color online) ROIs of the pyramidal tract (py), tectospinal tract (ts), and the trigeminothalamic tract (tth) overlaid on anatomical images. ROIs were drawn to be exclusive to the identified structure regardless of which rat they were placed on. All ROIs were of identical shape and size. The left and right ROIs were always placed along the same horizontal axis though the distance between the left and right ROIs varied across animals.

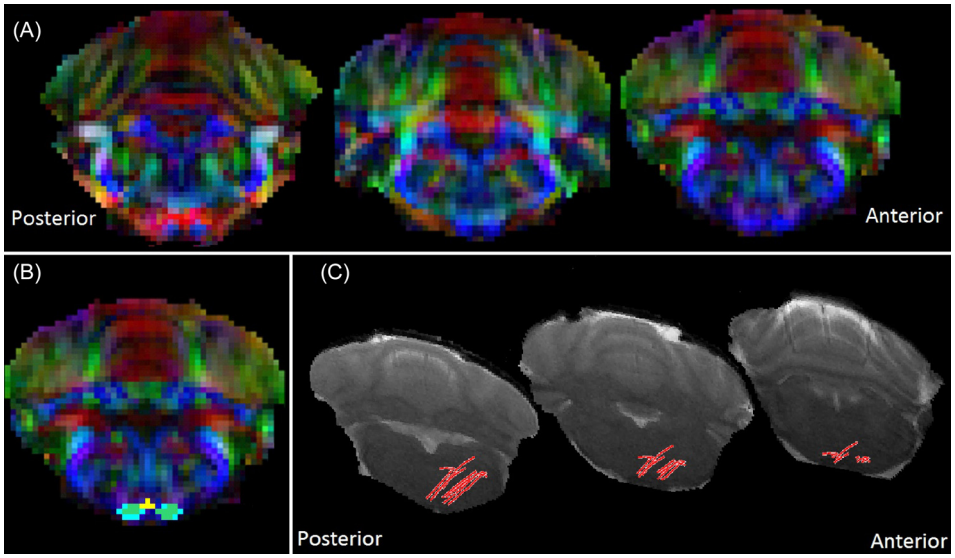

FIG. 4. (Color online) (A) Color-coded FA map of the second, third, and fourth coronal slices of the template rat that was subsequently used for normalization. Green: left-to-right; red: rostral-to-caudal; blue: dorsal-to-ventral of a rat brain in three orthogonal planes. (B) The second slice of the ROI of the pyramidal tract and the second slice of the voxel-based analysis results of the pyramidal tract are shown overlaid on the corresponding slice of the color map. The ROI is shown in light blue, the voxel-based analysis is shown in golden, and regions of overlap between the two are shown in green. The voxels selected by the voxel-based and ROI analyses overlap considerably. (C) Tracts were generated by seeding voxels from the pyramidal tract ROI with a minimum FA of 0.4 and terminating tracts that have an FA less than 0.2 or make more than a 60° turn. Fibers originating from the pyramidal tract ROI can be seen coursing through slices 2, 3, and 4 along the natural direction of the pyramidal tract.

of the VBS, highlighting clusters in which there are at least 50 contiguous significant voxels ($p < 0.0005$). VBS identified the pyramidal tract in slice 2 (−11.09 mm from bregma at its origin caudal to the longitudinal fasciculus) and slice 3 (−9.91 mm from bregma) throughout 73 voxels. The trigeminothalamic tract was identified in slice 2 at −11.09 mm from bregma throughout 81 voxels and the tectospinal tract was identified in slice 3 at −9.91 mm from bregma throughout 84 voxels.

Table I shows the statistics of each VBS cluster. The values and comparisons of MD, RD, and AD are shown for illustrative purposes but were not part of the analysis. *P*-values were computed by applying the *t*-test to the voxels of the images. Means were calculated by averaging the average value-per-voxel of each of the eight rats in each cohort. The uncorrected sample standard deviation was calculated using the average value-per-voxel of each of the eight rats in each cohort. In the pyramidal tract, FA was 0.40 ± 0.05 in the exposure rats and 0.20 ± 0.05 in the control rats ($p < 0.00005$), MD was 0.88 ± 0.20 in the exposure rats, and 1.48 ± 0.11 in the control rats ($p < 0.00005$). In the trigeminothalamic tract, FA was 0.20 ± 0.04 in the exposure rats and 0.39 ± 0.05 in the control rats ($p < 0.00005$). In the tectospinal tract, FA was 0.20 ± 0.03 in the exposure rats and 0.32 ± 0.03 in the control rats ($p < 0.00005$).

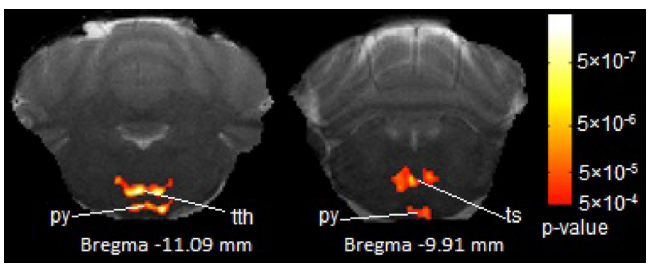

FIG. 5. (Color online) Clusters identified by VBS to contain significant differences in FA between the control and exposure groups are overlaid onto anatomical images. Clusters contain at least 50 voxels each with $p < 0.0005$. The pyramidal tract (py) consisting of 73 voxels, tectospinal tract (ts) consisting of 81 voxels, and the trigeminothalamic tract (tth) consisting of 84 voxels were identified.

The results of the ROI analysis are displayed in Table II, which compares the mean values of FA, MD, RD, and AD of the exposure and control rats in the pyramidal tract, tectospinal tract, and trigeminothalamic tract. Averages, standard deviation, and significance were calculated the same way for ROIs as they had been for clusters. In the pyramidal tract, FA was 0.47 ± 0.01 in the exposure rats and 0.45 ± 0.01 in the control rats ($p < 0.05$). In the trigeminothalamic tract, MD was 0.70 ± 0.02 in the exposure rats and 0.74 ± 0.02 in the control rats ($p < 0.005$).

There were no conflicting statistically significant ROI comparisons and VBS cluster comparisons. There were several conflicts in which one test yielded a statistically significant comparison but the other test yielded a non-statistically significant conflicting comparison. In the VBS comparison of the trigeminothalamic tract, FA was 0.20 ± 0.04 in the exposure rats and 0.39 ± 0.05 in the control rats ($p < 0.00005$); whereas in the ROI comparison FA was 0.34 ± 0.03 in the exposure rats and 0.32 ± 0.04 in the control rats (not significant). In the VBS comparison of the tectospinal tract, FA was 0.20 ± 0.03 in the exposure rats and 0.32 ± 0.03 in the control rats ($p < 0.00005$); whereas in the ROI comparison FA was 0.28 ± 0.02 in the exposure rats and 0.26 ± 0.02 in the control rats (not significant).

Both the color map and tractography (Fig. 4) confirm that the pyramidal tract region selected by VBS and further examined by ROI analysis is the pyramidal tract. The color map shows that the main direction of the FA eigenvector in

TABLE I. Diffusion tensor parameters of the clusters identified by VBS. Data are given as (mean ± standard deviation). $p < 0.05$, $p < 0.005$, and $p < 0.00005$ are indicated by *, **, and ***, respectively. p-values were computed by applying the t-test to the voxels of the images. Means were calculated by averaging the average value-per-voxel of each of the eight rats in each cohort. The uncorrected sample standard deviation was calculated using the average value-per-voxel of each of the eight rats in each cohort.

	Pyramidal tract		Trigeminothalamic tract		Tectospinal tract	
Structure	Control	Exposure	Control	Exposure	Control	Exposure
FA	0.20 ± 0.05	0.40 ± 0.05***	0.39 ± 0.05	0.20 ± 0.04***	0.32 ± 0.03	0.20 ± 0.03***
MD	1.48 ± 0.11	0.88 ± 0.20***	0.78 ± 0.07	0.74 ± 0.02	0.74 ± 0.01	0.71 ± 0.02*
RD	1.34 ± 0.13	0.66 ± 0.21***	0.60 ± 0.05	0.61 ± 0.16	0.62 ± 0.01	0.59 ± 0.15
AD	1.75 ± 0.10	1.26 ± 0.25**	1.14 ± 0.13	0.88 ± 0.03**	0.98 ± 0.04	0.86 ± 0.03***

the region of the pyramidal tract is along the posterior–anterior direction, consistent with the anatomy of the pyramidal tract. Similarly, in the tractography panel, the fibers originating from the ROIs course posterior–anterior in a bilaterally symmetrical fashion. In addition, the voxels selected by the VBS analysis overlap considerably with voxels selected by the ROI analysis.

IV. DISCUSSION

A. Neuroanatomical changes

VBS analysis of the DTI maps of exposure and control rats identified several regions within the medulla oblongata where FA significantly changed following long-term and passive acoustic exposure at moderate SPL. Specifically, VBS of the FA maps identified clusters overlaying the pyramidal tract as having significantly increased FA and clusters overlaying the tectospinal tract and trigeminothalamic tract as having significantly decreased FA in exposure rats compared to control rats. In both rodents and humans, the function of the pyramidal, trigeminothalamic, and tectospinal tract are the same. The pyramidal tract allows for voluntary control of the body and limbs, the trigeminothalamic tract is a somatosensory pathway that transmits noxious stimuli from the face, and the tectospinal tract is a motor pathway which reflexively controls the muscles of the head to react to visual stimuli. ROI analysis demonstrated significantly ($p < 0.05$) higher FA in the pyramidal tract of exposure rats than control rats. ROI analysis did not show significantly different FA of the trigeminothalamic tract or tectospinal tract of the exposure rats than control rats. The ROI analysis supported the observation of the VBS analysis that FA increased in the pyramidal tract following exposure. Our results showed that long-term and passive acoustic exposure at moderate SPL increased the organization of white matter in the pyramidal tract.

B. The medulla oblongata

The observed changes were contained to the medulla oblongata. The medulla oblongata has no known role in auditory processing as the auditory pathway is thought to enter the central nervous system superiorly at the pons. The current literature about the auditory system has focused on structures in the superior parts of the brain such as the inferior colliculus, anterior commissure, medial geniculate nucleus, and cochlear nucleus.[35,36] However, the current understanding of auditory pathways is generally based on human neuroanatomy and since rodents have different neuroanatomy and a more robust sense of hearing, it is possible that rodent auditory pathways have synapses in the medulla oblongata.

TABLE II. Diffusion tensor parameters of the ROIs. Data are given as (mean ± standard deviation). $p < 0.05$, $p < 0.01$, and $p < 0.005$ are indicated by *, **, and ***, respectively. p-values were computed by applying the t-test to the average values across all voxels in each ROI. Means were calculated by averaging the average value-per-voxel of each of the eight rats in each cohort. The uncorrected sample standard deviation was calculated using the average value-per-voxel of each of the eight rats in each cohort.

		Pyramidal tract		Trigeminothalamic tract		Tectospinal tract	
Structure		Control	Exposure	Control	Exposure	Control	Exposure
FA	Left	0.45 ± 0.02	0.47 ± 0.02	0.32 ± 0.04	0.35 ± 0.03	0.26 ± 0.03	0.28 ± 0.02
	Right	0.45 ± 0.02	0.47 ± 0.01*	0.31 ± 0.04	0.34 ± 0.04	0.27 ± 0.03	0.27 ± 0.02
	Both	0.45 ± 0.01	0.47 ± 0.01*	0.32 ± 0.04	0.34 ± 0.03	0.26 ± 0.02	0.28 ± 0.02
MD	Left	0.88 ± 0.09	0.86 ± 0.10	0.74 ± 0.02	0.70 ± 0.01***	0.72 ± 0.01	0.70 ± 0.03
	Right	0.86 ± 0.10	0.85 ± 0.12	0.74 ± 0.02	0.69 ± 0.03**	0.72 ± 0.01	0.70 ± 0.03
	Both	0.87 ± 0.09	0.86 ± 0.11	0.74 ± 0.02	0.70 ± 0.02***	0.72 ± 0.01	0.70 ± 0.03
RD	Left	0.66 ± 0.07	0.63 ± 0.06	0.61 ± 0.02	0.57 ± 0.02***	0.62 ± 0.02	0.60 ± 0.03
	Right	0.65 ± 0.08	0.63 ± 0.08	0.61 ± 0.04	0.57 ± 0.04	0.62 ± 0.01	0.60 ± 0.04
	Both	0.65 ± 0.07	0.63 ± 0.07	0.61 ± 0.03	0.57 ± 0.03**	0.62 ± 0.01	0.60 ± 0.03
AD	Left	1.32 ± 0.15	1.32 ± 0.18	1.00 ± 0.07	0.96 ± 0.04	0.91 ± 0.03	0.91 ± 0.04
	Right	1.28 ± 0.15	1.30 ± 0.19	0.98 ± 0.05	0.94 ± 0.03	0.93 ± 0.04	0.90 ± 0.04
	Both	1.30 ± 0.15	1.31 ± 0.19	0.99 ± 0.06	0.95 ± 0.03	0.92 ± 0.03	0.90 ± 0.03

An explanation consistent with the current understanding of neuroanatomy is that the changes in the medulla oblongata are a result of psychomotor agitation resulting from chronic stress induced by long-term and passive acoustic exposure. In humans, long-term and passive acoustic exposure at moderate SPL has been shown to induce a stress response as evident by cardiovascular, hormonal, and cognitive changes.[37–39] Long-term acoustic exposure at high SPL has been shown to cause oxidative stress and hormonal elevation in rats.[40,41] Chronic stress causes a number of symptoms including psychomotor agitation. Long-term and passive acoustic exposure at moderate SPL may be inducing chronic stress in adult rats resulting in psychomotor agitation. Increased white matter integrity of the pyramidal tract may result from the increased motor activity associated with psychomotor agitation as white matter integrity has been shown to correlate with the level of motor activity.[42,43]

C. Diffusion tensor imaging studies

There have been several DTI studies comparing the white matter tracts of musicians with non-musicians in which the pyramidal tract was identified as a key sensorimotor pathway. One study examined DTI maps from 26 musicians and 13 non-musicians and found decreased FA in the pyramidal tract of musicians compared to non-musicians.[44] In addition, a DTI study comparing five adults with musical training with seven adults without musical training also found decreased FA in the pyramidal tract of musicians.[45] However, a DTI study comparing eight male, right-handed professional pianists with eight age-matched non-musicians found higher FA in the pyramidal tract of musicians than non-musicians.[46] When analyzing these studies collectively, it appears that long-term musical practice is associated with decreased FA of the pyramidal tract.

Our study showed that long-term and passive acoustic exposure increased FA and decreased MD while musical training decreased FA and increased MD. As mentioned in Sec. I, long-term and passive acoustic exposure have a seemingly opposite electrophysiological and behavioral effect than long-term acoustic exposure coupled with behavioral training. Our study can be compared with those done on musicians as individuals who have undergone musical training have been exposed to a process which couples long-term acoustic exposure with behavioral training. When comparing the DTI studies on musicians with our DTI study on rats exposed to long-term and passive acoustic exposure, it can be inferred that neuroanatomically, long-term acoustic exposure coupled with behavioral training and long-term and passive acoustic exposure have opposite effects on the pyramidal tract and possibly other parts of the central nervous system.

DTI studies have also been performed on blast-induced brain injury in the auditory system of mice. These studies found decreased FA and increased apparent diffusion coefficient which were attributed with decreased axonal integrity and increased myelin injury, respectively. A number of studies in humans have found a positive correlation between the FA of the auditory system and age, with the common conclusion that increased FA reflects increased organization and development.[47] A study conducted on individuals who had suffered blast-related traumatic injury found that the FA of the pyramidal tract was positively correlated with total words recalled while apparent diffusion coefficient of the uncinate fasciculi and posterior internal capsule was negatively correlated with verbal memory.[48]

D. Technical considerations

Given the small relatively size of the rodent brain compared to the human brain, structures that would normally comprise thousands of voxels in a human brain imaged using similar MRI techniques will measure only a few voxels in the rodent brain. Therefore, even with optimal spatial normalization, it is a challenge for VBS to detect changes in structures such as the rodent pyramidal tract which spans just a couple of voxels in diameter. Therefore, we performed confirmatory ROI analysis as ROI analysis is not dependent on spatial normalization.

The observed white matter changes began gradually in the third slice and increased in the second slice. The first slice was not available for analysis due to post-processing but had it been available, the changes may have continued to occur caudally down the brainstem. Due to the frequent joining and branching of neurons in and out of the white matter tracts of the medulla oblongata, it is also possible that the changes were only observable at our conservative significance threshold ($p < 0.0005$) within a short segment of white matter.

Our methodology performed many comparisons with a conservative threshold for statistical significance whereas other studies performed a limited number of comparisons but with a lower threshold for statistical significance.[49,50] Therefore, we anticipate that our study will not detect minor changes in the sparse white matter fibers underlying gray matter auditory structures (such as the inferior colliculus and auditory cortex) but may detect major changes in previously unexamined white matter tracts.

V. CONCLUSION

DTI revealed greater FA of the pyramidal tract in rats receiving long-term and passive acoustic exposure. Our results suggest that long-term and passive acoustic exposure may have an opposite neuroanatomical effect than long-term acoustic exposure coupled with behavioral training, as inferred from musician studies. The changes were confined to the medulla oblongata indicating that long-term and passive acoustic exposure may cause changes in motor tracts through secondary behavioral changes. Further research should investigate the role of the medulla oblongata in the auditory system, sensorimotor training, and sensory adaptation.

ACKNOWLEDGMENTS

This research was supported by the Hong Kong General Research Fund (No. 661313), the Hong Kong Health and Medical Research Fund (No. 11122581), and start-up funding from the City University of Hong Kong.

[1]G. Andersson, "Psychological aspects of tinnitus and the application of cognitive–behavioral therapy," Clin. Psychol. Rev. **22**(7), 977–990 (2002).
[2]J. J. Eggermont and L. E. Roberts, "The neuroscience of tinnitus," Trends Neurosci. **27**(11), 676–682 (2004).
[3]I. C. Bruce, M. B. Sachs, and E. D. Young, "An auditory-periphery model of the effects of acoustic trauma on auditory nerve responses," J. Acoust. Soc. Am. **113**(1), 369–388 (2003).
[4]S. G. Kujawa and M. C. Liberman, "Adding insult to injury: Cochlear nerve degeneration after 'temporary' noise-induced hearing loss," J. Neurosci. **29**(45), 14077–14085 (2009).
[5]B. Hassfurth, A. K. Magnusson, B. Grothe, and U. Koch, "Sensory deprivation regulates the development of the hyperpolarization-activated current in auditory brainstem neurons," European J. Neurosci. **30**(7), 1227–1238 (2009).
[6]A. Kral and J. J. Eggermont, "What's to lose and what's to learn: Development under auditory deprivation, cochlear implants and limits of cortical plasticity," Brain Res. Rev. **56**(1), 259–269 (2007).
[7]A. Kral, R. Hartmann, J. Tillein, S. Heid, and R. Klinke, "Congenital auditory deprivation reduces synaptic activity within the auditory cortex in a layer-specific manner," Cerebral Cortex **10**(7), 714–726 (2000).
[8]E. F. Chang and M. M. Merzenich, "Environmental noise retards auditory cortical development," Science **300**(5618), 498–502 (2003).
[9]A. Muzet, "Environmental noise, sleep and health," Sleep Med. Rev. **11**(2), 135–142 (2007).
[10]D. B. Polley, E. E. Steinberg, and M. M. Merzenich, "Perceptual learning directs auditory cortical map reorganization through top-down influences," J. Neurosci. **26**(18), 4970–4982 (2006).
[11]H. Nakahara, L. I. Zhang, and M. M. Merzenich, "Specialization of primary auditory cortex processing by sound exposure in the 'critical period,' " Proc. Natl. Acad. Sci. U.S.A. **101**(18), 7170–7174 (2004).
[12]V. Scheper, G. Paasche, J. M. Miller, A. Warnecke, N. Berkingali, T. Lenarz, and T. Stöver, "Effects of delayed treatment with combined GDNF and continuous electrical stimulation on spiral ganglion cell survival in deafened guinea pigs," J. Neurosci. Res. **87**(6), 1389–1399 (2009).
[13]X. Zhou and M. M. Merzenich, "Environmental noise exposure degrades normal listening processes," Nature Commun. **3**, 843 (2012).
[14]C. Lau, M. Pienkowski, J. W. Zhang, B. McPherson, and E. X. Wu, "Chronic exposure to broadband noise at moderate sound pressure levels spatially shifts tone-evoked responses in the rat auditory midbrain," NeuroImage **122**, 44–51 (2015).
[15]C. Lau, J. W. Zhang, B. McPherson, M. Pienkowski, and E. X. Wu, "Long-term, passive exposure to non-traumatic acoustic noise induces neural adaptation in the adult rat medial geniculate body and auditory cortex," NeuroImage **107**, 1–9 (2015).
[16]F. Gao, J. Zhang, X. Sun, and L. Chen, "The effect of postnatal exposure to noise on sound level processing by auditory cortex neurons of rats in adulthood," Physiol. Behav. **97**(3), 369–373 (2009).
[17]J. Xu, L. Yu, R. Cai, J. Zhang, and X. Sun, "Early continuous white noise exposure alters auditory spatial sensitivity and expression of GAD65 and GABAA receptor subunits in rat auditory cortex," Cerebral Cortex **20**(4), 804–812 (2010).
[18]W. Sun, L. Tang, and B. L. Allman, "Environmental noise affects auditory temporal processing development and NMDA-2B receptor expression in auditory cortex," Behav. Brain Res. **218**(1), 15–20 (2011).
[19]D. Le Bihan, "Looking into the functional architecture of the brain with diffusion MRI," Nature Rev. Neurosci. **4**(6), 469–480 (2003).
[20]D. J. Mabbott, M. Noseworthy, E. Bouffet, S. Laughlin, and C. Rockel, "White matter growth as a mechanism of cognitive development in children," Neuroimage **33**(3), 936–946 (2006).
[21]T. Klingberg, M. Hedehus, E. Temple, T. Salz, J. D. Gabrieli, M. E. Moseley, and R. A. Poldrack, "Microstructure of temporo-parietal white matter as a basis for reading ability: Evidence from diffusion tensor magnetic resonance imaging," Neuron. **25**(2), 493–500 (2000).
[22]M. Shenton, H. Hamoda, J. Schneiderman, S. Bouix, O. Pasternak, Y. Rathi, M. A. Vu, M. P. Purohit, K. Helmer, I. Koerte, and A. P. Lin, "A review of magnetic resonance imaging and diffusion tensor imaging findings in mild traumatic brain injury," Brain Imag. Behav. **6**(2), 137–192 (2012).
[23]Y. Chang, S. H. Lee, Y. J. Lee, M. J. Hwang, S. J. Bae, M. N. Kim, J. Lee, S. Woo, H. Lee, and D. S. Kang, "Auditory neural pathway evaluation on sensorineural hearing loss using diffusion tensor imaging," Neuroreport **15**(11), 1699–1703 (2004).
[24]F. T. Husain, R. E. Medina, C. W. Davis, Y. Szymko-Bennett, K. Simonyan, N. M. Pajor, and B. Horwitz, "Neuroanatomical changes due to hearing loss and chronic tinnitus: A combined VBM and DTI study," Brain Res. **1369**, 74–88 (2011).
[25]S. H. Lee, Y. Chang, J. E. Lee, and J. H. Cho, "The values of diffusion tensor imaging and functional MRI in evaluating profound sensorineural hearing loss," Cochlear Implants Int. **5**(Supplement-1), 149–152 (2004).
[26]H. J. Kim, C. G. Choi, D. H. Lee, J. H. Lee, S. J. Kim, and D. C. Suh, "High-b-value diffusion-weighted MR imaging of hyperacute ischemic stroke at 1.5 T," Am. J. Neurorad. **26**(2), 208–215 (2005).
[27]J. C. Mao, E. Pace, P. Pierozynski, Z. Kou, Y. Shen, P. VandeVord, E. M. Haacke, X. Zhang, and J. Zhang, "Blast-induced tinnitus and hearing loss in rats: Behavioral and imaging assays," J. Neurotrauma **29**(2), 430–444 (2012).
[28]S. K. Song, S. W. Sun, W. K. Ju, S. J. Lin, A. H. Cross, and A. H. Neufeld, "Diffusion tensor imaging detects and differentiates axon and myelin degeneration in mouse optic nerve after retinal ischemia," Neuroimage **20**(3), 1714–1722 (2003).
[29]S. W. Sun, H. F. Liang, K. Trinkaus, A. H. Cross, R. C. Armstrong, and S. K. Song, "Noninvasive detection of cuprizone induced axonal damage and demyelination in the mouse corpus callosum," Magnetic Reson. Med. **55**(2), 302–308 (2006).
[30]Y. Lin, J. Wang, C. Wu, Y. Wai, J. Yu, and S. Ng, "Diffusion tensor imaging of the auditory pathway in sensorineural hearing loss: Changes in radial diffusivity and diffusion anisotropy," J. Magnetic Reson. Imag. **28**(3), 598–603 (2008).
[31]C. M. Wu, S. H. Ng, J. J. Wang, and T. C. Liu, "Diffusion tensor imaging of the subcortical auditory tract in subjects with congenital cochlear nerve deficiency," Am. J. Neuroradiol. **30**(9), 1773–1777 (2009).
[32]See supplementary material at http://dx.doi.org/10.1121/1.4972300 for the results of ABRs recorded from one control and one noise exposed (2 months, 65 dB SPL) subject. The thresholds for the two subjects were both close to 5 dB and thus, no clinically significant threshold shift was observed.
[33]G. Paxinos and C. Watson, *The Rat Brain in Stereotaxic Coordinates* (Academic Press, Cambridge, 2006), 456 pp.
[34]E. S. Hui, M. M. Cheung, K. C. Chan, and E. X. Wu, "B-value dependence of DTI quantitation and sensitivity in detecting neural tissue changes," Neuroimage **49**(3), 2366–2374 (2010).
[35]C. Alain, S. R. Arnott, S. Hevenor, S. Graham, and C. L. Grady. " 'What' and 'where' in the human auditory system," Proc. Natl. Acad. Sci. U.S.A. **98**(21), 12301–12306 (2001).
[36]D. A. Bulkin and J. M. Groh, "Seeing sounds: Visual and auditory interactions in the brain," Curr. Opinion Neurobiol. **16**(4), 415–419 (2006).
[37]E. Franssen, C. Van Wiechen, N. Nagelkerke, and E. Lebret, "Aircraft noise around a large international airport and its impact on general health and medication use," Occupat. Environ. Med. **61**(5), 405–413 (2004).
[38]C. Maschke, J. Harder, H. Ising, K. Hecht, and W. Thierfelder, "Stress hormone changes in persons exposed to simulated night noise," Noise Health **5**(17), 35–45 (2002).
[39]S. A. Stansfeld and M. P. Matheson, "Noise pollution: Non-auditory effects on health," British Med. Bull. **68**(1), 243–257 (2003).
[40]A. Anthony, E. Ackerman, and J. A. Lloyd, "Noise stress in laboratory rodents. I. Behavioral and endocrine response of mice, rats, and guinea pigs," J. Acoust. Soc. Am. **31**(11), 1430–1437 (1959).
[41]S. Manikandan and R. S. Devi, "Antioxidant property of α-asarone against noise-stress-induced changes in different regions of rat brain," Pharmacol. Res. **52**(6), 467–474 (2005).
[42]S. Walther, A. Federspiel, H. Horn, N. Razavi, R. Wiest, T. Dierks, W. Strik, and T. J. Müller, "Alterations of white matter integrity related to motor activity in schizophrenia," Neurobiol. Disease **42**(3), 276–283 (2011).
[43]H. Johansen-Berg, V. Della-Maggiore, T. E. Behrens, S. M. Smith, and T. Paus, "Integrity of white matter in the corpus callosum correlates with bimanual co-ordination skills," Neuroimage **36**, T16–T21 (2007).
[44]A. Imfeld, M. S. Oechslin, M. Meyer, T. Loenneker, and L. Jancke, "White matter plasticity in the corticospinal tract of musicians: A diffusion tensor imaging study," Neuroimage **46**(3), 600–607 (2009).
[45]V. J. Schmithorst and M. Wilke, "Differences in white matter architecture between musicians and non-musicians: A diffusion tensor imaging study," Neurosci. Lett. **321**(1), 57–60 (2002).
[46]S. L. Bengtsson, Z. Nagy, S. Skare, L. Forsman, H. Forssberg, and F. Ullén, "Extensive piano practicing has regionally specific effects on white matter development," Nat. Neurosci. **8**(9), 1148–1150 (2005).
[47]K. M. Kennedy and N. Raz, "Aging white matter and cognition: Differential effects of regional variations in diffusion properties on

memory, executive functions, and speed," Neuropsychologia **47**(3), 916–927 (2009).
[48]H. S. Levin, E. Wilde, M. Troyanskaya, N. J. Petersen, R. Scheibel, M. Newsome, M. Radaideh, T. Wu, R. Yallampalli, Z. Chu, and X. Li, "Diffusion tensor imaging of mild to moderate blast-related traumatic brain injury and its sequelae," J. Neurotrauma **27**(4), 683–694 (2010).
[49]L. G. Astrakas and M. I. Argyropoulou, "Shifting from region of interest (ROI) to voxel-based analysis in human brain mapping," Pediatric Radiol. **40**(12), 1857–1867 (2010).
[50]L. Snook, C. Plewes, and C. Beaulieu, "Voxel based versus region of interest analysis in diffusion tensor imaging of neurodevelopment," Neuroimage **34**(1), 243–252 (2007).